Virtual Electrode Effects in Myocardial Fibers

Stephen B. Knisley, Bruce C. Hill, and Raymond E. Ideker
Department of Biomedical Engineering and the Engineering Research Center in Emerging Cardiovascular Technologies, School of Engineering, Duke University, Durham, North Carolina 27710, and Research Institute, Palo Alto Medical Foundation, Palo Alto, California, USA

ABSTRACT The changes in transmembrane potential during a stimulation pulse in the heart are not known. We have used transmembrane potential sensitive dye fluorescence to measure changes in transmembrane potential along fibers in an anisotropic arterially perfused rabbit epicardial layer. Cathodal or anodal extracellular point stimulation produced changes in transmembrane potential within 60 μm of the electrode that were positive or negative, respectively. The changes in transmembrane potential did not simply decrease to zero with increasing distance, as would occur with a theoretical fiber space constant, but instead became reversed beyond approximately 1 mm from the electrode consistent with a virtual electrode effect. Even stimulation from a line of terminals perpendicular to the fibers produced negative changes in transmembrane potential for cathodal stimulation with the largest negative changes during a 50-ms pulse at 3–4 mm from the electrode terminals. Negative changes as large as the amplitude of the action potential rising phase occurred during a 50-ms pulse for 20-volt cathodal stimulation. Switching to anodal stimulation reversed the directions of changes in transmembrane potential at most recording spots, however for stimulation during the refractory period negative changes in transmembrane potential were significantly larger than positive changes in transmembrane potential. Anodal stimulation during diastole with 3-ms pulses produced excitation in the region of depolarization that accelerated when the stimulation strength was increased to >3 times the anodal threshold strength. Thus, virtual electrode effects of unipolar stimulation occur in myocardial fibers, and for sufficiently strong stimuli the virtual electrode effects may influence electrical behavior of the myocardium.

INTRODUCTION

Extracellular electrical stimulation is commonly used in cardiac pacing and antiarrhythmic electrical therapy such as defibrillation and cardioversion. The process of extracellular electrical stimulation is thought to involve first the induced changes in transmembrane potentials during the stimulation pulse and then activation of transmembrane voltage-dependent ion channels, e.g., sodium channels that conduct inwardly directed current. Although the latter effect has been extensively studied in excitable membranes, e.g., using voltage clamp techniques or activation mapping techniques, the induced changes in transmembrane potentials during extracellular stimulation pulses have not been extensively studied. Data exists for induced changes in transmembrane potentials during extracellular stimulation pulses in isolated one-dimensional myocardial fibers (e.g., Weidmann, 1970) in which the fiber space constant was measured, however, very little data exists for two-dimensional myocardium or hearts (Dillon and Wit, 1988; Tung and Neunlist, 1992). Whether the stimulation-induced changes in transmembrane potential in hearts are consistent with the fiber space constant has never been tested.

Theoretical and experimental studies of two-dimensional anisotropic myocardium with unequal resistance anisotropy ratios for the intracellular and extracellular spaces have indicated a complex spatial distribution of induced changes in transmembrane potentials during current injection or extracellular stimulation (Sepulveda et al., 1989; Wikswo et al., 1991). The theoretical study (Sepulveda et al., 1989) predicted that 1) a region of change in transmembrane potential with a "dogbone" shape extends in the direction transverse to the fibers, which was verified experimentally using excitation measurements (Wikswo et al., 1991), 2) current loops in anisotropic myocardium (Plonsey and Barr, 1984) produce a measurable magnetic field, which has been experimentally confirmed (Staton et al., 1991; Staton et al., 1993), and 3) the transmembrane potential at different locations along the myocardial fibers is shifted in one direction very near a unipolar stimulation electrode, while it is shifted in the opposite direction a short distance away from the electrode. This is markedly different from some predictions of one-dimensional models in which the direction of the change in transmembrane potential is not reversed, but instead the change in transmembrane potential decreases to zero as one moves away from the electrode (Weidmann, 1970; Hodgkin and Rushton, 1946). Measurements that could test the predictions of the distribution of changes in transmembrane potential during a stimulation pulse in the heart have not been reported.

Such measurements are difficult to obtain with conventional techniques. For example, microelectrode recordings from tissue in an electric field can contain an undesired stimulation artifact or deflection during the stimulation pulse that does not represent a change in transmembrane potential. This artifact has been minimized in experiments with isolated heart tissue by carefully adjusting the relative positions of extracellular and intracellular electrodes in the stimulation field (Knisley et al., 1992*a*). The difficulty of obtaining many intracellular measurements with this technique limits the ability to measure a distribution of changes in transmembrane potential. Therefore we used transmembrane voltage-sensitive dye fluorescence that follows changes in

Received for publication 8 July 1993 and in final form 13 December 1993.
Address reprint requests to Stephen B. Knisley, Ph.D., P.O. Box 3140, Duke University Medical Center, Durham, NC 27710.

0006-3495/94/03/719/10 $2.00

transmembrane potential and, in some experiments, a laser scanner system that provides fluorescence recordings at many sites simultaneously. To allow our results to be compared qualitatively with the predictions of two-dimensional theoretical models we used an endocardially prefrozen rabbit heart preparation, which provided an approximately two-dimensional layer of arterially perfused anisotropic epicardium.

METHODS

Experiments were performed with seven isolated rabbit hearts endocardially prefrozen with liquid nitrogen as described (Allessie et al., 1989; Hill et al., 1990) to produce a 1-mm layer of surviving epicardium. The hearts were Langendorff-perfused with Tyrode's solution at 36–37°C and an aortic pressure of 50 mm Hg containing 129 mM NaCl, 4.5 mM KCl, 1.8 mM $CaCl_2$, 1.1 mM $MgCl_2$, 14 mM $NaHCO_3$, 1 mM Na_2HPO_4, 11 mM glucose, 40 mg/L bovine serum albumin (Sigma Chemical Co., St. Louis, MO) and bubbled with 95:5% O_2/CO_2 and having a pH of 7.3 to 7.4. Diacetyl monoxime was added at a concentration of 20 mM to eliminate contraction artifacts in the optical recordings (Li et al., 1985). The hearts were stained with a voltage-sensitive fluorescent dye, either di-4-ANEPPS (Molecular Probes, Inc., Eugene, OR) for 2 min at a concentration of 0.01 mg/mL added to the perfusate in dye-saturated ethanol (Fluhler et al., 1985) or WW781 added to the perfusate at a concentration of 0.005 mg/mL.

In experiments with a fluorescence microscope, an approximately 100-μm region of the heart was illuminated by a 514-nm argon laser beam (Model 532 Omnichrome, Chino, CA) focused by an objective lens with a numerical aperture of 0.25. The laser intensity reaching the hearts stained with di-4-ANEPPS was approximately 0.25 mW. Fluorescence collected by the objective lens passed through a dichroic beamsplitter and longpass glass filter with a cutoff wavelength of 570 nm and a magnifying lens to produce an overall magnification in the image plane of 25×. The change in intensity of the fluorescence light from the cell membrane followed the transmembrane voltage of the cells (Ehrenberg et al., 1987; Windisch et al., 1991; Knisley et al., 1993). The fluorescence light emitted from a 60-μm diameter region of the epicardium was measured in the image plane with an avalanche photodiode having an active diameter of 1.5 mm. The amount of fluorescence light emitted from the 60-μm diameter region was small, which limited the signal-to-noise ratio. The di-4-ANEPPS produces a larger change in the collected fluorescence during an action potential rising phase than WW781 (unpublished results), which helped in discerning transmembrane potentials from the small region. The recordings were stored on a digitizing oscilloscope (Norland, Madison, WI) at a sampling rate of 2 kHz.

In other experiments simultaneous action potentials were recorded optically with a computer-controlled laser scanner system previously described in which the laser beam was steered with acousto-optic modulators (Hill and Courtney, 1987). A beam from a 647-nm krypton laser (Model 95k, Lexel, Fremont, CA) with an intensity of 7 mW scanned a portion of the left ventricular epicardium of hearts stained with WW781 illuminating a 9-mm square grid of 64 recording spots 100 μm in diameter. The fluorescence light passed through a 665-nm longpass filter and was collected with a photomultiplier tube. The fluorescence recording was demultiplexed by the computer into individual action potential recordings from each spot. The sampling rate for each spot was 1 kHz.

The direction of the fastest propagation, which was assumed coincident with the fiber axis in the mapped region, was determined by stimulating at the center of the grid during diastole and evaluating the long axis of elliptical isochrones. The grid was then rotated so that one side of the grid was perpendicular to the long axis of the elliptical isochrones.

The heart was paced with a bipolar electrode on the left ventricle. The test stimulation was then applied on the left ventricle 1–10 mm from the pacing site. The test stimulation electrode was either a single 25-μm diameter electrode (Fig. 1) or a line of electrodes made of 125-μm diameter wire bent through 180 degrees near the end and fed through two preformed holes in flexible silicone ribbon. The outer surface of the bend contacted the heart. The ribbon was mounted on a sponge and gentle pressure was applied to fit the contour of the epicardial surface. The line was oriented perpendicular to the epicardial fibers (Fig. 4). A 1–2-cm^2 sponge return electrode was positioned on the side of the heart opposite the stimulation electrode.

The electric field strength produced by the test stimulation from the line of electrodes was measured in the center of the scanned region with fine wire recording electrodes approximately 2 mm apart. The distance between the recording electrodes was measured before and after each experiment with a microscope and reticle. The voltages were passed through a wideband differential isolation amplifier (Analog Devices AD210AN) and stored on a digitizing oscilloscope (Model 1425 Gould Electronics, Valley View, OH) with a sampling rate >20 kHz. The electric field magnitude was determined by dividing the differential voltage by the interelectrode distance. Contour maps of changes in transmembrane potential produced by test stimulation were generated by a computerized contour fitting program (Golden Software Inc., Golden, CO) using the regional variable theory technique of Kriging (Ripley, 1981).

The times of tissue excitation at individual recording spots in the scanned region were studied for anodal or cathodal stimulation applied in diastole from the line of electrodes. The stimulation pulse had a duration of 3 ms and strength that ranged from below the threshold up to the strength that produced an electric field of 1.6 V/cm in the center of the scanned region. Excitation times at the recording spots were determined as the time of the midpoint of the fast rising phase of the action potential as previously described (Spach and Kootsey, 1985; Hill et al., 1990).

Combined results are given as the mean ± 1 SD. Two-tailed t tests were used to evaluate the statistical significance of the changes in transmembrane potential and the differences in changes in transmembrane potential at two given distances from the stimulation electrode.

RESULTS

Changes in transmembrane potential within 1 mm of a point stimulation electrode during a stimulation pulse

Fluorescence recordings were obtained immediately adjacent to a point stimulation electrode (0 mm), 0.5 and 1 mm away from the electrode (Fig. 1). The hearts were S1 paced from an electrode at the left side of the heart, and then S2 test stimulation was applied in the refractory period or diastolic period from a point stimulation electrode. Each recording contained an S1-induced action potential rising phase that could be used as an approximate calibration for the changes in transmembrane potential that occur later in the recording. For S2 in the refractory period, the tissue was refractory to S2 so that the active responses were partly suppressed, which may reveal passive responses of the tissue. Because nonlinear membrane behavior still exists, responses were not strictly passive responses. Fig. 2 shows fluorescence recordings obtained at different distances from the cathodal point stimulation electrode in three trials in one rabbit heart. The point stimulation electrode location on the epicardium and the stimulation current strength and polarity were constant in the three trials, but the fluorescence recording location under the objective lens was changed between trials by moving the heart and stimulation electrode as a single unit. The action potential rising phase produced by the S1 stimulation is shown in the left part of each fluorescence recording. The S2 stimulation pulse was given at an S1-S2 interval of 75 ms.

The 60-μm diameter recording region of the myocardium adjacent to the cathodal S2 point stimulation electrode (recording labeled 0 mm in Fig. 2) became depolarized during the 2-ma S2 pulse. The peak magnitude of this depolarization was 55% of the action potential rising phase amplitude. At 0.5 mm away from the S2 electrode, the myocardium became

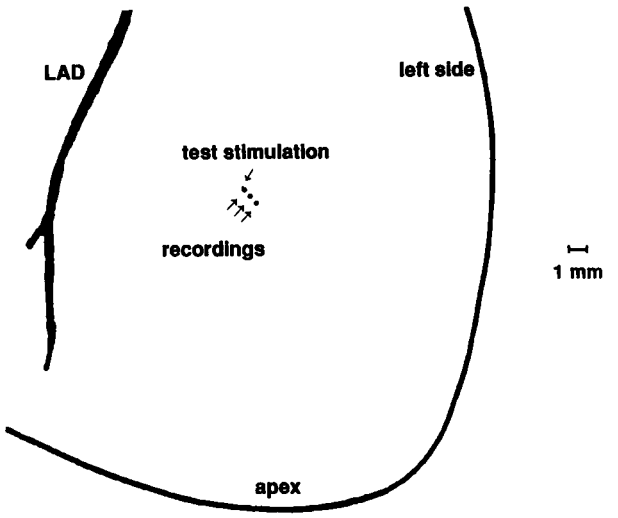

FIGURE 1 Enlarged diagram of the anterior left ventricle showing the region of test S2 point stimulation and the recording spots in experiments with the fluorescence microscope. The test stimulation was applied from a 25-μm diameter wire electrode, too small to see in the diagram (see *downward-oriented arrow* pointing toward stimulation site). Fluorescence recordings were obtained from three 60-μm diameter recording sites on the epicardium (see spots with the three parallel *arrows* pointing to them) that were immediately adjacent to the test stimulation electrode (0 mm), 0.5 mm away and 1 mm away from the electrode. The line containing recording spots and stimulation spot was parallel to the direction of fastest propagation. The left anterior descending artery is shown in the left part of the diagram. The outline of the left side and apex of the heart is shown in the right and bottom parts of the diagram.

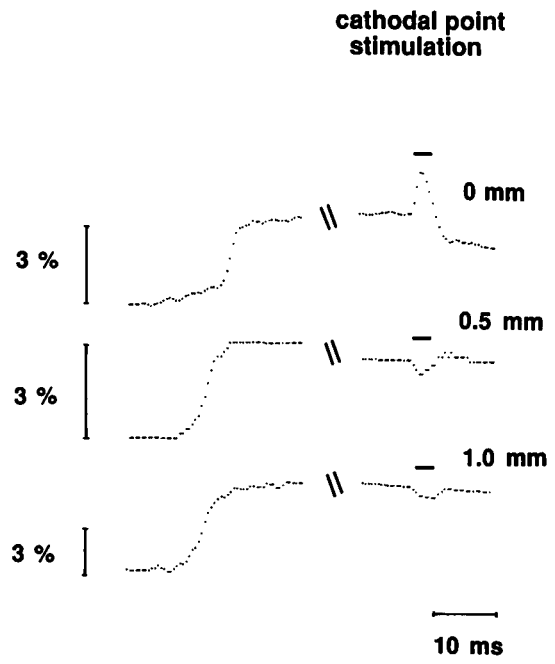

FIGURE 2 Fluorescence recordings obtained at different distances from a cathodal point stimulation electrode. The fluorescence recordings are interrupted where indicated by the double slashes after the rising phases, and then begin again 25 ms after the interruption. The duration of the stimulation pulse is indicated by the horizontal mark above each fluorescence recording. The myocardium adjacent to the electrode (0 mm) became depolarized during the stimulation pulse. At 0.5 mm away from the electrode, the myocardium became hyperpolarized during the pulse. At 1.0 mm away from the electrode, the myocardium became hyperpolarized during the pulse. Calibration bars on the left indicate the percent of the total fluorescence. The effect of the fluorescence decrease because of photobleaching of the fluorescent dye was eliminated by linear subtraction. Stimulation pulse strength was 2 ma.

hyperpolarized during a 2-ma S2 stimulation pulse. The peak magnitude of this hyperpolarization during the pulse was 15% of the action potential rising phase amplitude. Also at 1.0 mm away from the electrode, the myocardium became hyperpolarized during a 2-ma S2 stimulation pulse. The peak magnitude of the hyperpolarization at 1.0 mm was 11% of the action potential rising phase amplitude. Other trials showed that the direction of the transmembrane potential change at a given recording location during S2 could be reversed by reversing the S2 stimulation polarity.

Results from a different heart in which anodal point S2 stimulation was given in diastole after the S1-induced action potential are shown in Fig. 3. A 1-ma anodal S2 produced hyperpolarization at 0 mm from the S2 point stimulation electrode during the S2 pulse. A transmembrane potential change produced by a 1-ma anodal S2 at 0.5 mm from the electrode was not discerned above the noise level. A transmembrane potential change produced by a 1-ma anodal S2 at 1 mm from the electrode (not shown) was not discerned above the noise level. A 2-ma anodal S2 produced the depolarization shown in Fig. 3 at 1 mm.

Changes in transmembrane potential 1 to 10 mm from a line stimulation electrode during a stimulation pulse

In five other hearts we examined a region approximately 1 to 10 mm away from a line of S2 electrode terminals (Fig. 4). The experiments described above indicated that with an S2 current of 2 ma, which was less than the diastolic anodal point stimulation threshold, the magnitude of the change in transmembrane potential 1 mm away from the electrode was only a small fraction of the action potential rising phase amplitude and could be difficult to discern in our fluorescence recordings. Increasing the S2 strength can increase the magnitude of change in transmembrane potential (Knisley et al., 1993), however, even though we saw no large changes in the diastolic threshold that may indicate tissue damage after applying S2 current of 2 ma, we considered that a large increase in the S2 strength may damage the small electrode or the tissue (e.g., a 2-ma S2 produces a current density of 407 a/cm^2 at the tip of the electrode assuming a uniform current density). In other experiments we used a line of S2 stimulation electrode terminals oriented perpendicular to the fibers (Fig. 4) and constant voltage stimulation applied at all the terminals at once. This electrode had sufficient area of contact with the tissue to allow S2 as strong as 10–30 times the diastolic threshold without producing the high current density described. Also, the use of the line of electrodes instead of a point electrode produced a larger fraction of current in the direction along fibers, which we thought may allow us to determine both the space constant along fibers in the heart and the electric field strength required to directly excite the

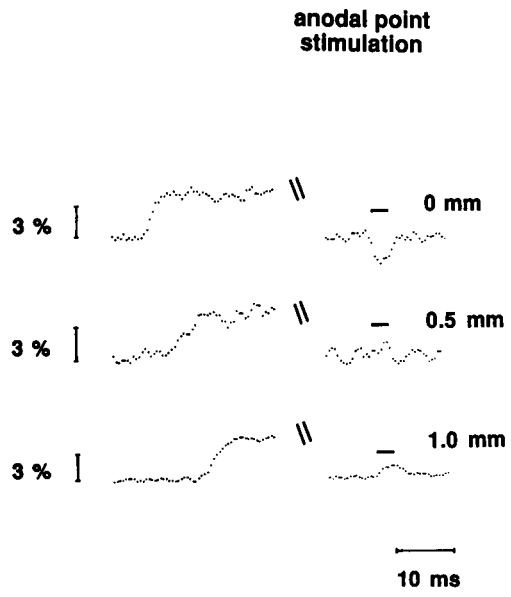

FIGURE 3 Fluorescence recordings obtained at different distances from an anodal point stimulation electrode. The fluorescence recordings are interrupted where indicated by the double slashes after the rising phases and then begin again 225 ms after the interruption. The duration of the stimulation pulse is indicated by the horizontal mark above each fluorescence recording. The myocardium adjacent to the electrode (0 mm) became hyperpolarized during the stimulation pulse. At 1.0 mm away from the electrode the myocardium became depolarized during the pulse. The calibration bars on the left indicate the percent of the total fluorescence. The effect of the fluorescence decrease because of photobleaching of the fluorescent dye was eliminated by linear subtraction. Stimulation pulse strength was 1 ma for recordings at 0 and 0.5 mm and 2 ma for the recording at 1 mm.

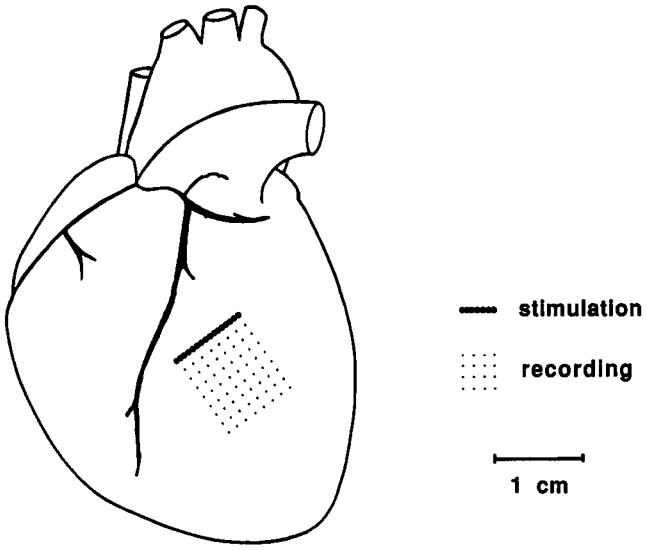

FIGURE 4 Diagram of heart showing the S2 stimulation location and laser scanner recording region on the anterior left ventricle. The S2 stimulation was applied from a line of terminals perpendicular to the epicardial fibers. Simultaneous fluorescence recordings were obtained from 64 spots in a 9- × 9-mm region beginning approximately 1 mm from the S2 stimulation electrode.

myocardial fibers, which has been evaluated in the heart using extracellular but not transmembrane potential recordings (Frazier et al., 1988). In each heart, a laser scanner system was used to obtain simultaneous fluorescence recordings at 64 spots in a region adjacent to the electrode terminals.

Fig. 5 *A* shows the fluorescence recordings from a trial in which cathodal stimulation with a strength of 20 V was used. The S1 stimulation was applied approximately 1 mm to the reader's left of the recordings. The times of the S1 and the S2 stimuli, respectively, are indicated by the small vertical and horizontal marks above the recordings. The S2 pulse duration was 50 ms, so that the changes in transmembrane potential during the pulse could be easily discerned. The S2 was applied at an S1-S2 interval of 40 ms. The recordings show two action potentials induced by S1 stimuli without S2, and then one with S2. For each recording spot, the changes in transmembrane potential induced by the S2 were evaluated as the fluorescence at the end of the S2 pulse minus the fluorescence measured at the same time after S1 in a preceding action potential without S2. This difference was expressed as a fraction of the fluorescence change during the rising phase of the S1-induced action potential without S2. At a given spot the action potentials without S2 were nearly identical. Thus the changes in transmembrane potential during the S2 pulse were not the result of beat-to-beat variations among the action potentials produced by S1 without S2. The changes in transmembrane potential along the fibers induced by S2 did not exhibit a space constant predicted from some one-dimensional models, i.e., a decrease from a maximum depolarization near the electrode to zero away from the electrode. Instead, hyperpolarization during the cathodal S2 occurred at all spots except spot 0, which was approximately 10 mm away from the S2 stimulation electrode. Hyperpolarization occurred both where the S2 pulse began during the rising phase of the S1-induced action potential (e.g., spots 53 and 61) and where the pulse began at the completion of the rising phase (e.g., spots 5 and 13). Changes in transmembrane potential at the 64 recording spots were different at different distances from the S2 stimulation electrode. In the top row of spots, changes in transmembrane potential as fractions of the amplitudes of action potential rising phases were -0.34 ± 0.1. Changes in transmembrane potential increased at spots farther from the electrode, reaching a maximum of -0.88 ± 0.14 in the fourth row from the electrode (distance between rows = 1.3 mm). Moving still farther from the electrode, changes in transmembrane potential decreased to -0.46 ± 0.28 in the eighth row, i.e., the row farthest from the electrode. A contour map of the changes in transmembrane potential induced by the cathodal S2 (Fig. 5 *B*) shows the distribution of hyperpolarization within the scanned region.

Fig. 6 *A* shows fluorescence recordings from the same region and with the same S2 strength as in the previous figure, however the S2 polarity was switched so that the S2 electrode was an anode. At 57 of the 64 recording sites the direction of the change in the transmembrane potential induced by S2 was reversed by reversing the polarity of the stimulation, whereas at 7 of the 64 sites (spots 23, 31, 39, 47,

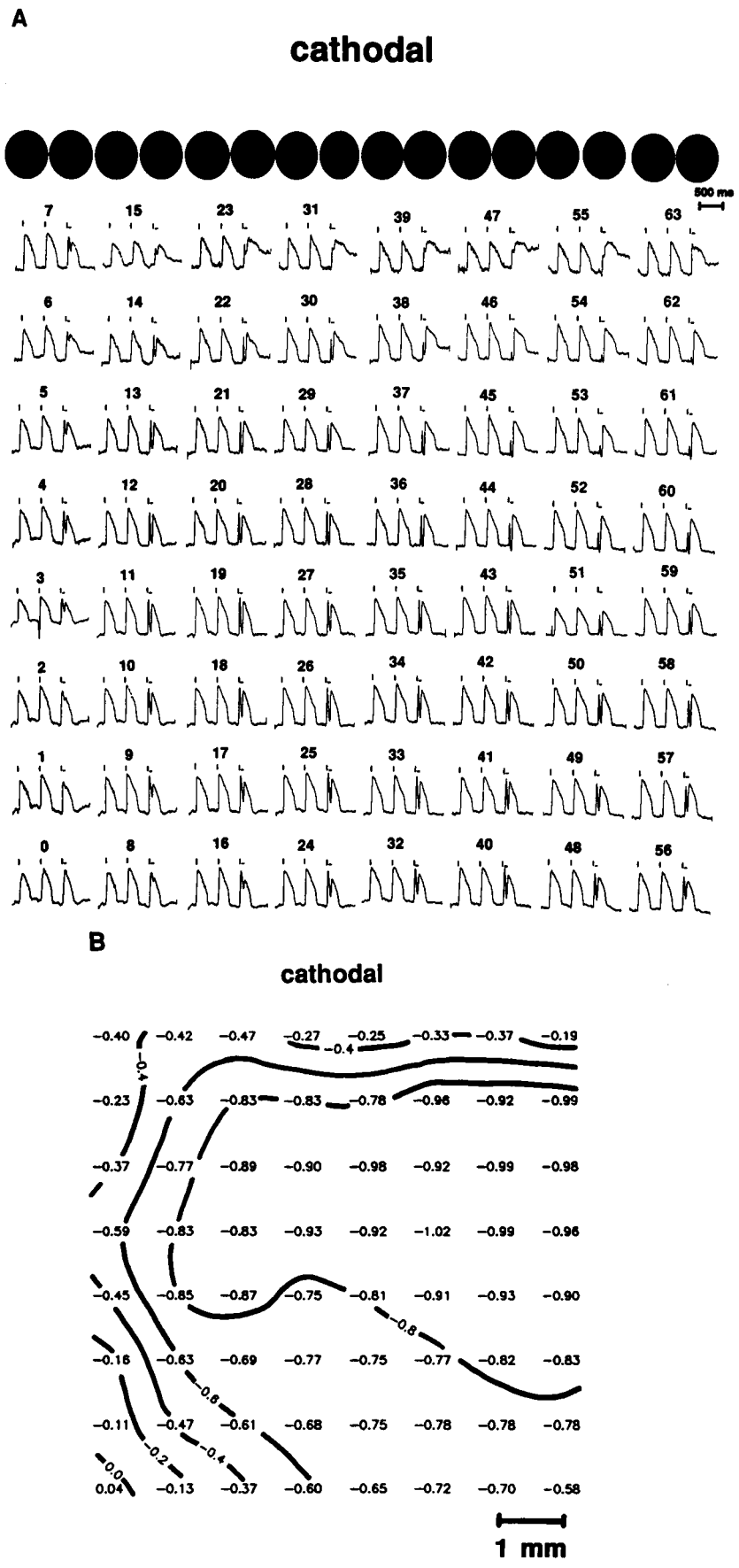

FIGURE 5 Fluorescence recordings showing effect of a cathodal stimulation pulse in a region adjacent to a stimulation electrode, and contour plot showing spatial distribution of changes in transmembrane potential induced during the pulse. (*A*) Spatial arrangement of recordings corresponds to recording spots in Fig. 4. Each recording shows two S1-induced action potentials produced by pacing with an S1 electrode that was to the reader's left of the recording region and then a third S1-induced action potential during which an S2 stimulation pulse was applied from a line of electrode terminals (row of large *spots*) illustrated above the recording region. Hyperpolarization during the S2 pulse occurred at all spots except spot 0; (*B*) Contour plot showing the distribution of hyperpolarization in the recording region. The hyperpolarization at each recording spot is given as a fraction of the amplitude of the S1-induced action potential rising phase. Contour lines are shown at intervals of 0.2 times the amplitude of the action potential rising phase.

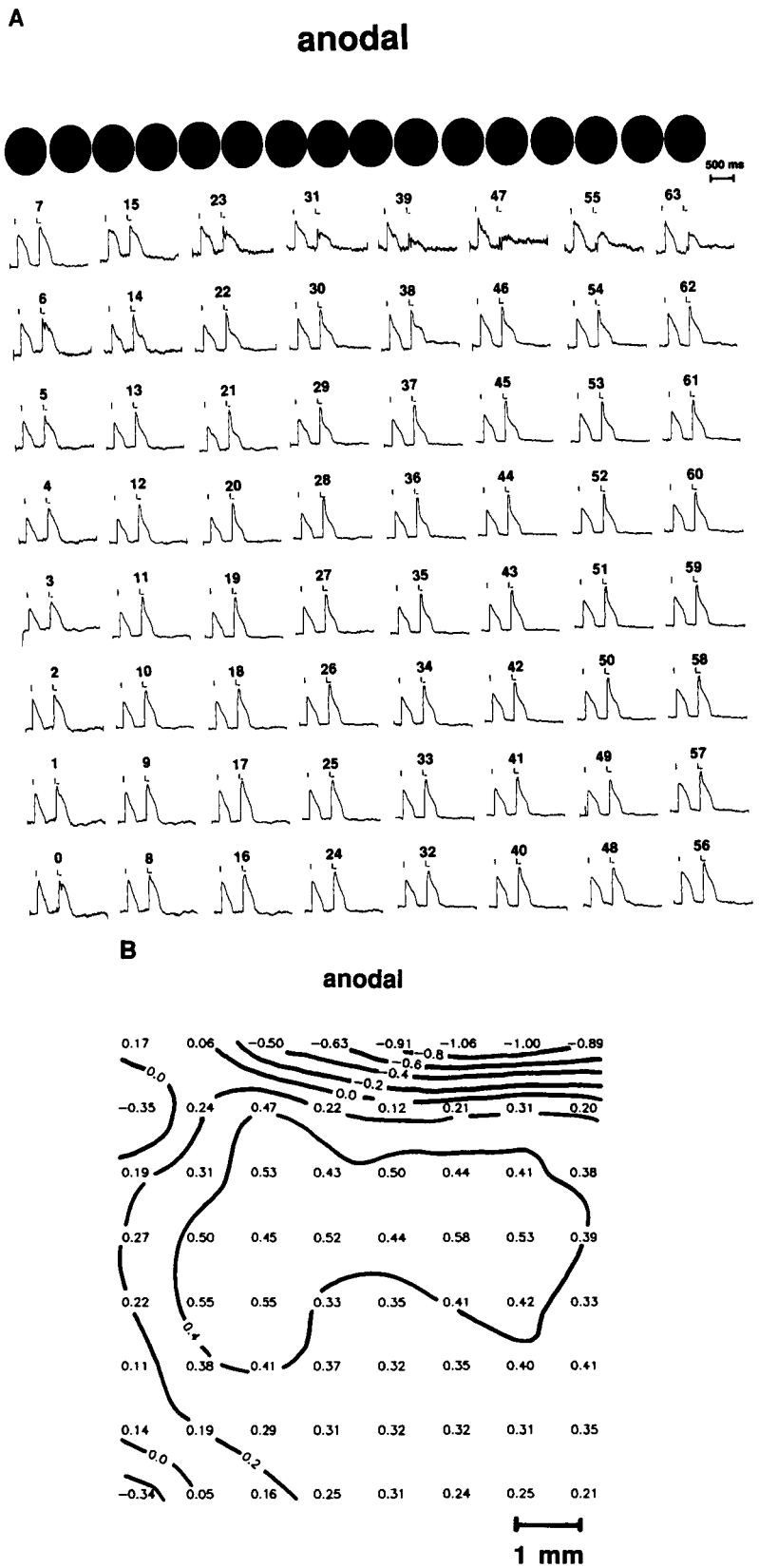

FIGURE 6 Fluorescence recordings from the same region and with the same S2 strength as in Fig. 5 but with an anodal stimulation pulse and contour plot of changes in transmembrane potential induced during the pulse. (*A*) Each recording shows an S1-induced action potential without an S2 stimulation pulse and then an S1-induced action potential during which an S2 stimulation pulse was applied from a line of electrode terminals (row of large *spots*) illustrated above the recording region. Positive changes in transmembrane potential, i.e., depolarization, during S2 occurred at most spots; (*B*) Contour plot showing the distribution of depolarization in the recording region. The depolarization at each recording spot is given as a fraction of the amplitude of the S1-induced action potential rising phase. Contour lines are shown at intervals of 0.2 times the amplitude of the action potential rising phase.

55, 63, and 6) the direction of the change in transmembrane potential remained negative for both S2 polarities. Six of these seven sites were in the top row. The changes in transmembrane potential at two spots in the top row during the anodal pulse were positive (spots 7 and 15). The action potential plateau in the top row after the end of the S2 pulse was

typically much more negative than the plateau without S2 (spots 23, 31, 39, 47, 55, and 63). At spots in the second row, except spot 14, the direction of transmembrane potential change induced by S2 was the opposite of the direction at the corresponding spot in the first row. In the second row, changes in transmembrane potential as fractions of the amplitudes of action potential rising phases were 0.18 ± 0.24. In rows farther from the electrode, changes in transmembrane potential became larger, reaching 0.46 ± 0.1 in the fourth row. Moving still farther from the electrode, changes in transmembrane potential decreased to 0.14 ± 0.21 in the eighth row, i.e., the row farthest from the electrode. A contour map (Fig. 6 *B*) shows the distribution of changes in transmembrane potential induced by the anodal S2. The location of the region of depolarization induced by the anodal S2 almost matched the location of the region of hyperpolarization induced by the cathodal S2 shown in Fig. 5 *B*.

The magnitudes of the negative changes in transmembrane potential at a given spot were larger than the magnitudes of the positive changes that occurred after the S2 polarity was reversed. This is clearly seen in the fourth row where the negative changes induced by the cathodal S2 (Fig. 5) averaged 91% larger than the positive changes induced by the anodal S2 (Fig. 6).

Fig. 7 shows the changes in transmembrane potential as a function of distance along the fibers in three hearts in which the S2 duration was 50 ms and strength was 16 ± 5 V. For each distance in each heart, the measurements from the two central columns of recording spots were averaged. The changes in transmembrane potential increased significantly with distance to approximately the center of the recording region (p = 0.011 for cathodal and p = 0.016 for anodal fourth row versus first row, n = 3 hearts). Beyond the center the changes in transmembrane potential decreased with distance from the electrode (p = 0.020 for cathodal and p = 0.069 for anodal eighth row versus fourth row, n = 3 hearts). The magnitudes of changes in transmembrane potential induced by S2 were greater for cathodal than for anodal S2 stimulation (p = 0.009 anodal versus cathodal for all distances from the electrode combined in three hearts, n = 24).

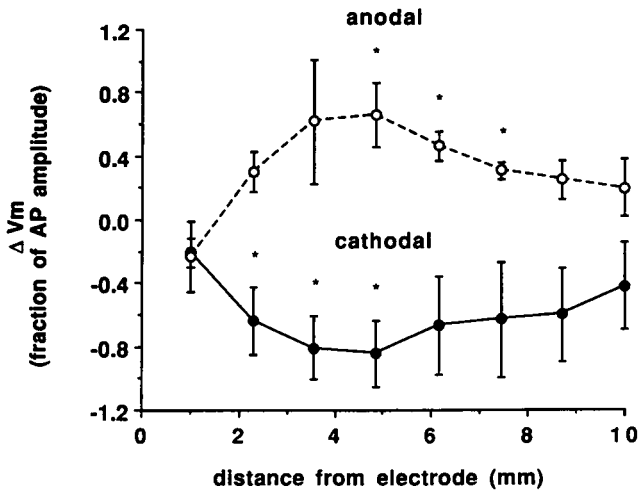

FIGURE 7 Changes in transmembrane potential during S2 stimulation pulses expressed as fractions of amplitudes of S1-induced action potential rising phases (ΔV_m) versus distance along the fibers in three hearts in which the S2 duration was 50 ms and strength was 16 ± 5 V. S2 was applied from a line of terminals perpendicular to the epicardial fibers. The magnitude of ΔV_m increased and then decreased with distance from the electrode terminals. Magnitudes of ΔV_m were greater for cathodal than for anodal stimulation. * = $p < 0.05$ ΔV_m versus zero, n = 3

In two other hearts, 6 V cathodal S2 pulses with durations of 5 or 15 ms were tested. With these weaker stimuli, hyperpolarization was discerned above the noise level at some spots away from the electrode. In the central columns of the recording region in these hearts, the largest hyperpolarizations as fractions of the amplitudes of the action potential rising phases were approximately −0.2 and occurred approximately 3 mm from the electrode.

In three of the five hearts studied with the laser scanner (one heart with a 15-ms and 6-V S2 and two hearts with a 50-ms and approximately 16-V S2), the cathodal S2 induced positive changes in transmembrane potential at one or more spots in the top row (approximately 1 mm from the S2 electrode). In all five hearts combined, the cathodal S2 induced positive changes in transmembrane potential at 40% of the recording spots in the top row, whereas the other spots in the top row underwent negative changes in transmembrane potential or no change. For all rows in all five hearts combined, the cathodal S2 induced hyperpolarization at 60% of all of the recording spots (65% of the recording spots if just spots in the two central columns are counted). The location relative to the S2 electrode of the largest magnitude of hyperpolarization in the two central columns was 3.6 ± 1 mm from the electrode.

Excitation after stimulation

We considered that brief stimulation pulses given in diastole may induce changes in transmembrane potential that are important for cardiac pacing. For example, during anodal stimulation cells away from the electrode may be temporarily depolarized toward the threshold transmembrane potential for membrane excitation, which may alter velocity of an excitation front passing through the region after the stimulation pulse either by decreasing the amount of further depolarization needed to attain threshold or by producing delayed direct excitation away from the electrode (Krassowska et al., 1992). On the other hand depolarization during the pulse may inactivate voltage-dependent sodium channels (e.g., Fozzard and Arnsdorf, 1991), which may decrease membrane excitability and propagation velocity after the pulse.

In two hearts, we examined excitation and propagation produced by stimulation in diastole with a 3-ms pacing pulse applied from the line of S2 electrode terminals. Fig. 8 shows an example in one heart of the effect of increasing the stimulation strength from 2 to 3.5 V (4 to 7 times the cathodal threshold strength or 1.8 to 3.2 times the anodal threshold strength) on the excitation times along the fibers in the center of the scanned region. The two stimulation strengths produced epicardial electric fields of 0.9 V/cm or 1.6 V/cm in

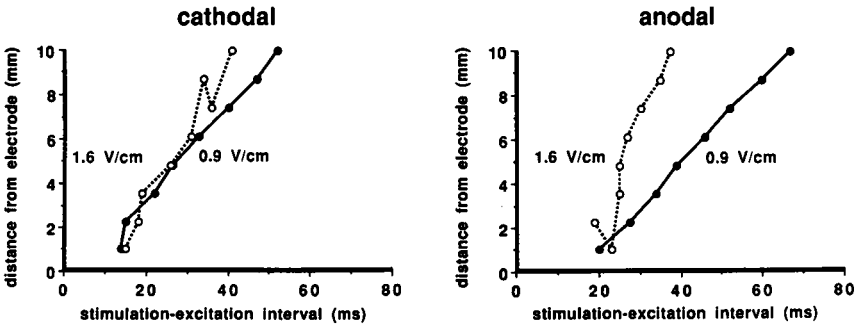

FIGURE 8 Plots of the distance from the stimulation electrode measured along epicardial fibers in the center of the scanned region versus the interval from the onset of the stimulation pulse to excitation (stimulation-excitation interval). The 3-ms stimulation pulse was applied in diastole from a line of terminals perpendicular to the epicardial fibers (same electrode used in Figs. 4–7). The effect of increasing the stimulation strength is shown for cathodal stimulation (*left graph*) and anodal stimulation (*right graph*). Increasing the cathodal stimulation strength from 2 to 3.5 V, which increased the epicardial electric field in the center of the scanned region from 0.9 V/cm (*solid lines*) to 1.6 V/cm (*dotted lines*), produced an increase in the longitudinal propagation velocity away from the electrode from 22 to 32 cm/s. For anodal stimulation, such an increase in the stimulation strength produced an increase in longitudinal propagation velocity from 19 to 47 cm/s.

the center of the scanned region. The earliest excitation in the scanned region occurred at least approximately 10 ms after the end of the pulse. For the weaker pulse of either polarity, earliest excitation occurred at the site closest to the electrode and propagated away from the electrode. The stronger anodal pulse produced earlier excitation and faster propagation at sites away from the electrode. Linear regressions of the excitation times versus distance provided intercepts of regression lines with the distance axis and velocity estimates (i.e., slope of linear regression) dominated by the propagation away from the electrode. The intercept is a measure of the apparent point of origin of propagation for which a negative value implies excitation latency. The intercepts for the data in Fig. 8 were −1.3 and −3.4 mm for the weaker and stronger cathodal pulses, respectively. The intercepts were −2.9 and −7.9 mm for the weaker and stronger anodal pulses. The longitudinal propagation velocity for cathodal stimulation increased from 22 cm/s ($r^2 = 0.987$) to 32 cm/s ($r^2 = 0.955$) when the stimulation strength was increased. The increase in the stimulation strength for anodal stimulation yielded a longitudinal propagation velocity increase from 19 cm/s ($r^2 = 0.998$) to 47 cm/s ($r^2 = 0.882$). Results from another heart were qualitatively consistent with the increased propagation velocity with increased anodal stimulation strength shown.

DISCUSSION

Previous experimental data has described changes in the transmembrane potential during an extracellular stimulation pulse in one-dimensional myocardial preparations. Those results, which agree with theoretical results during a stimulation pulse in a one-dimensional cable (Weidmann, 1970; Hodgkin and Rushton, 1946; Jack et al., 1983), indicate that the transmembrane potential is depolarized near the cathodal electrode and hyperpolarized near the anodal electrode and that the magnitudes of the changes in transmembrane potential are greatest near the electrode and decrease exponentially to zero with increasing distance from the electrode. The exponential decrease has allowed determinations of the fiber space constant.

Our results indicate that in the preparation studied, some of the changes in transmembrane potential differ from those seen in one-dimensional preparations. Like the results from one-dimensional preparations, we observed depolarization very near the cathodal electrode and that the depolarization became smaller moving away from the electrode. In our experiments with the laser scanner (Figs. 4–7) the recording spots in most of the recording region were too far away from the electrode to see this depolarization, but in our experiments with the microscope (Figs. 1–3), which provided recordings near and immediately adjacent to the electrode, this depolarization was apparent. However, unlike the results from one-dimensional preparations, our experiments with both the scanner and the microscope showed that at spots away from the electrode hyperpolarization was produced by cathodal stimulation and depolarization was produced by anodal stimulation. At distances from the electrode greater than a few mm, the magnitude of the hyperpolarization produced by cathodal stimulation increased with distance, reached a maximum at approximately 4 mm, and then decreased with distance (Fig. 7). Thus, the changes in transmembrane potential were not consistent with a decreasing exponential function and space constant predicted from classical one-dimensional theory.

The hyperpolarization that we observed for cathodal stimulation has been suggested by some theoretical results. A bidomain model of a two-dimensional myocardium with a ratio of the longitudinal to the transverse resistance in the intracellular space that is different from the ratio in the extracellular space has predicted that point stimulation with an extracellular cathodal electrode produces regions of hyperpolarization (virtual anodes) away from the electrode in the direction along the myocardial fibers (Sepulveda et al., 1989). Predictions from this model have been partially confirmed experimentally (Wikswo et al., 1991; Staton et al., 1991; Staton et al., 1993). Also a theoretical model that described an "activating function" has shown hyperpolarization during extracellular cathodal stimulation in a fiber bathed in conductive solution (Rattay, 1989). Although our results are

qualitatively consistent with these theoretical models, the accuracy of match between theory and experiment may be affected by differences between the models and the experimental preparation. For example, effects of current flowing in all three dimensions could contribute to our results.

Our results do not rule out a "sawtooth" pattern of depolarization and hyperpolarization that has been predicted to occur at the ends of cells in cardiac fibers during a stimulation pulse (Plonsey and Barr, 1986; Krassowska et al., 1987), and which has been observed at the ends of isolated ventricular myocytes in an electric field aligned with the myocyte (Knisley et al., 1993). The area of fluorescence collection in the present experiments encompassed many cell ends and hence, possible changes in transmembrane potential that are in opposite directions at the cell ends may be averaged in our recordings. The virtual electrode effects that we observed would theoretically be superimposed on any sawtooth pattern.

The changes in transmembrane potential induced by a pulse are not simply proportional to the applied stimulation voltage. We found that at some spots approximately 1 mm from the stimulation electrode the direction of the transmembrane potential remained negative (the hyperpolarizing direction) when the stimulation polarity was reversed (e.g., spots 23 and 31 in Figs. 5 and 6). Also, we found that for a given stimulation strength during the action potential plateau, the negative changes in transmembrane potential obtained with one stimulation polarity were significantly larger than the positive changes obtained with the other polarity (e.g., Fig. 7). This finding is consistent with earlier transmembrane potential measurements during polarizing pulses of either polarity given extracellularly during the action potential plateau in isolated ventricular fibers (Cranefield and Hoffman, 1958). Also, it is qualitatively consistent with the slightly larger negative changes than positive changes at the ends of isolated ventricular myocytes during electric field stimulation (Knisley et al., 1993).

Such nonproportionality of the changes in transmembrane potential to the stimulation strength may result from nonlinear membrane properties that occur normally, e.g., inward sodium current that produces a positive transmembrane potential change or outward potassium current, which produces a negative transmembrane potential change (Fozzard and Arnsdorf, 1991). Also it is possible that membrane damage occurs near the electrode, which may introduce abnormal membrane behavior.

We evaluated excitation in the scanned region after stimulation in diastole with 3-ms pulses having strengths that produced potential gradients in the center of the scanned region of up to 1.6 V/cm, similar to the potential gradient required to excite tissue (Frazier et al., 1988; Knisley et al., 1992*b*). The 20-mM diacetyl monoxime that we used to eliminate heart motion also decreases inward sodium current (Li et al., 1985), which should be considered in interpreting our excitation results. In our excitation experiments, the earliest excitation produced by the weaker of the two stimulation strengths occurred closer to the electrode than to the region away from the electrode where virtual electrode effects were measured. Thus for producing capture of the heart with the weaker stimulation strength, the transmembrane potential change during the stimulation pulse close to the electrode is more important than the virtual electrode effect or the existence of the extracellular electric field away from the electrode. This is consistent with our fluorescence microscope results, which showed much larger changes in transmembrane potential within 60 μm of the point electrode compared with 0.5 mm or 1 mm away from the electrode. However, for stronger anodal stimulation, virtual electrode effects may be important for the site of initiation of propagation. For example, the 1.6 V/cm anodal pulse in Fig. 8 produced earlier excitation 2 mm from the electrode compared with 1 mm from the electrode, which corresponds to a greater amount of depolarization at 2 mm from the electrode compared with 1 mm (Fig. 7).

The size of a virtual electrode region and the magnitude of the change in transmembrane potential in the region are predicted to increase with increases in the stimulation strength (Sepulveda et al., 1989). Therefore, the virtual electrode effects induced by a sufficiently strong stimulus may alter voltage-dependent membrane channels sufficiently to produce block, delayed propagation, or action potential repolarization changes that may contribute to reentry (Knisley et al., 1992*b*).

We observed faster propagation when the strength of the 3-ms anodal stimulation pulse was increased. The central region of the velocity measurement, i.e., the center of the recording region, was at the approximate location of the largest depolarization induced by anodal stimulation. This suggests that the depolarization may contribute to the faster propagation. It is conceivable that the excitability of the tissue away from the electrode was increased by summation of stimulatory effects of depolarization induced by the virtual electrode effect with stimulatory effects of local circuit currents of propagation. Slight membrane depolarization induced by a modest elevation of extracellular potassium has already been shown to both decrease the difference between the transmembrane potential and the threshold transmembrane potential for membrane excitation (Kishida et al., 1979) and produce faster propagation (Hiramatsu et al., 1989). Another possibility, which is suggested by our activation results in Fig. 8 for the 1.6-V/cm anodal pulse, is that the anodal pulse did not initiate propagation at the electrode, but instead the electric field produced delayed excitation in cells away from the electrode. The negative intercepts with the distance axis obtained in the linear regressions for the data in Fig. 8 and the individual measurements of the stimulation-excitation intervals indicate that excitation latency occurred. Excitation latency also occurs in isolated rabbit papillary muscles after electric field stimulation near the threshold strength (Knisley et al., 1992*a*) and has been attributed to sodium channel behavior in a theoretical model (Krassowska et al., 1992). For cathodal stimulation, no marked increase in propagation velocity with increased stimulation strength was observed, suggesting that hyper-

polarization in the region of the virtual electrode effect may not increase the propagation velocity.

Limitations

The current strength applied from the point stimulation electrode and electric field strength produced at the center of the scanned region by stimulation with the line of electrodes do not quantify currents responsible for the changes in transmembrane potential in different directions at different distances from the electrode. The experimental design is not optimal for testing the predictions of virtual electrode effects of point stimulation in two-dimensional anisotropic myocardium with unequal anisotropy (Sepulveda et al., 1989). This theory predicts that a reversal in the direction of the transmembrane potential change with increasing distance from the electrode occurs along fibers, which our experiments showed, but not across fibers, which we did not test. Also, the use of a line of electrodes in some of our experiments, which we used to test whether the space constant predicted from one-dimensional models occurs in our preparation, is not optimal to produce virtual electrode effects predicted for point stimulation.

We thank Wanda Krassowska and Lara G. Villanueva for assistance in preparing figures of the fluorescence recordings.

This research was supported by National Institutes of Health research grants HL-35216 of the National Heart, Lung and Blood Institute and BRSG S07 RR005513 of the Biomedical Research Support Grant Program, Division of Research Resources, National Science Foundation Engineering Research Center grant CDR-8622201, American Heart Association North Carolina Affiliate grant NC-91-G-14, North Carolina Biotechnology Center Grant 9113-ARG-0612, and a Grant from the Whitaker Foundation.

REFERENCES

Allessie, M. A., M. J. Schalij, C. J. H. J. Kirchhof, L. Boersma, M. Huybers, and J. Hollen. 1989. Experimental electrophysiology and arrhythmogenicity: anisotropy and ventricular tachycardia. *Eur. Heart J.* 10(Suppl E):2–8.

Cranefield, P. F., and B. F. Hoffman. 1958. Propagated repolarization in heart muscle. *J. Gen. Physiol.* 41:633–649.

Dillon, S. M., and A. L. Wit. 1988. Use of voltage sensitive dyes to investigate electrical defibrillation. *In* Proc. 10th Annual Conf. of the IEEE Engineering in Medicine and Biology Society. G. Harris, and C. Walker, editors. IEEE, Inc., New Orleans, LA. 0215–0216.

Ehrenberg, B., D. L. Farkas, E. N. Fluhler, Z. Lojewska, and L. M. Loew. 1987. Membrane potential induced by external electric field pulses can be followed with a potentiometric dye. *Biophys. J.* 51:833–837.

Fluhler, E., V. G. Burnham, and L. M. Loew. 1985. Spectra, membrane binding, and potentiometric responses of new charge shift probes. *Biochemistry* 24:5749–5755.

Fozzard, H. A., and M. F. Arnsdorf. 1991. Cardiac Electrophysiology. *In* The Heart and Cardiovascular System: Scientific Foundations. H. A. Fozzard, E. Haber, R. B. Jennings, A. M. Katz, and H. E. Morgan, editors. Raven Press, New York. 73–78.

Frazier, D. W., W. Krassowska, P.-S. Chen, P. D. Wolf, E. G. Dixon, W. M. Smith, and R. E. Ideker. 1988. Extracellular field required for excitation in three-dimensional anisotropic canine myocardium. *Circ. Res.* 63:147–164.

Hill, B. C., A. J. Hunt, and K. R. Courtney. 1990. Reentrant tachycardia in a thin layer of ventricular subepicardium: effects of *d*-sotalol and lidocaine. *J. Cardiovasc. Pharmacol.* 16:871–880.

Hill, B. C., and K. R. Courtney. 1987. Design of a multi-point laser scanned optical monitor of cardiac action potential propagation: application to microreentry in guinea pig atrium. *Ann. Biomed. Eng.* 15:567–577.

Hiramatsu, Y., J. W. Buchanan, Jr., S. B. Knisley, G. G. Koch, S. Kropp, and L. S. Gettes. 1989. Influence of rate-dependent cellular uncoupling on conduction change during simulated ischemia in guinea pig papillary muscles: effect of Verapamil. *Circ. Res.* 65:95–102.

Hodgkin, A. L., and W. A. H. Rushton. 1946. The electrical constants of a crustacean nerve fibre. *Proc. R. Soc. Lond. Ser. B Biol. Sci.* 133:444–479.

Jack, J. J. B., D. Noble, and R. W. Tsien. 1983. Electric Current Flow in Excitable Cells. Oxford University Press, Oxford. 413–422.

Kishida, H., B. Surawicz, and L. T. Fu. 1979. Effects of K^+ and K^+-induced polarization on $(dV/dt)_{max}$, threshold potential, and membrane input resistance in guinea pig and cat ventricular myocardium. *Circ. Res.* 44: 800–814.

Knisley, S. B., T. F. Blitchington, B. C. Hill, A. O. Grant, W. M. Smith, T. C. Pilkington, and R. E. Ideker. 1993. Optical measurements of transmembrane potential changes during electric field stimulation of ventricular cells. *Circ. Res.* 72:255–270.

Knisley, S. B., W. M. Smith, and R. E. Ideker. 1992*a* Effect of intrastimulus polarity reversal on electric field stimulation thresholds in frog and rabbit myocardium. *J. Cardiovasc. Electrophysiol.* 3:239–254.

Knisley, S. B., W. M. Smith, and R. E. Ideker. 1992*b* Effect of field stimulation on cellular repolarization in rabbit myocardium: Implications for reentry induction. *Circ. Res.* 70:707–715.

Krassowska, W., T. C. Pilkington, and R. E. Ideker. 1987. Periodic conductivity as a mechanism for cardiac stimulation and defibrillation. *IEEE Trans. Biomed. Eng.* 34:555–560.

Krassowska, W., C. Cabo, S. B. Knisley, and R. E. Ideker. 1992. Propagation versus delayed activation during field stimulation of cardiac muscle. *PACE* 15:197–210.

Li, T., N. Sperelakis, R. E. Teneick, and R. J. Solaro. 1985. Effects of diacetyl monoxime on cardiac excitation-contraction coupling. *J. Pharmacol. Exp. Ther.* 232:688–695.

Plonsey, R., and R. C. Barr. 1984. Current flow patterns in two-dimensional anisotropic bisyncytia with normal and extreme conductivities. *Biophys. J.* 45:557–571.

Plonsey, R., and R. C. Barr. 1986. Effect of microscopic and macroscopic discontinuities on the response of cardiac tissue to defibrillating (stimulating) currents. *Med. & Biol. Eng. & Comput.* 24:130–136.

Rattay, F. 1989. Analysis of models for extracellular fiber stimulation. *IEEE Trans. Biomed. Eng.* 36:676–682.

Ripley, B. D. 1981. Spatial Statistics. John Wiley & Sons, New York. 44–54.

Sepulveda, N. G., B. J. Roth, and J. P. Wikswo, Jr. 1989. Current injection into a two-dimensional anisotropic bidomain. *Biophys. J.* 55:987–999.

Spach, M. S., and J. M. Kootsey. 1985. Relating the sodium current and conductance to the shape of transmembrane and extracellular potentials by simulation: effects of propagation boundaries. *IEEE Trans. Biomed. Eng.* 32:743–755.

Staton, D. J., R. N. Friedman, and J. P. Wikswo, Jr. 1991. High-resolution squid magnetocardiographic mapping of action currents in canine cardiac slices. *Circulation* 84:II–667. (Abstr.)

Staton, D. J., R. N. Friedman, and J. P. Wikswo, Jr. 1993. High-resolution squid imaging of octupolar currents in anisotropic cardiac tissue. *IEEE Trans. Applied Superconductivity* 3:1934–1936.

Tung, L., and M. Neunlist. 1992. Regional depolarization of cardiac muscle adjacent to an epicardial stimulating anode. *Am. Heart J.* 124:834. (Abstr.)

Weidmann, S. 1970. Electrical constants of trabecular muscle from mammalian heart. *J. Physiol. (Lond.).* 210:1041–1054.

Wikswo, J. P., Jr., T. A. Wisialowski, W. A. Altemeier, J. R. Balser, H. A. Kopelman, and D. M. Roden. 1991. Virtual cathode effects during stimulation of cardiac muscle: Two-dimensional in vivo experiments. *Circ. Res.* 68:513–530.

Windisch, H., H. Ahammer, P. Schaffer, W. Müller, and B. Koidl. 1991. Optical multisite detection of membrane potentials in single cardiomyocytes during voltage clamp. *Proc. 13th Annual Conf. of the IEEE: Engineering in Medicine and Biology Society* 13:0605–0606.